

## SEMI-INTERPENETRATING NETWORK HYDROGELS BASED ON POLY(METHACRYLIC ACID) AND NATURAL POLYMERS GELATIN, CHITOSAN, AND ALGINATE FOR POTENTIAL BIOMEDICAL APPLICATIONS

Vukasin Ugrinovic<sup>1\*</sup>, Andjela Radisavljevic<sup>1</sup>, Maja Markovic<sup>1</sup>, Vesna Panic<sup>1</sup>, Djordje Veljovic<sup>2</sup>

<sup>1</sup>Innovation Center of the Faculty of Technology and Metallurgy, University of Belgrade, Belgrade, Serbia

<sup>2</sup>Faculty of Technology and Metallurgy, University of Belgrade, Belgrade, Serbia

\*vugrinovic@tmf.bg.ac.rs

Hydrogels, known for their high hydration, porosity, and permeability, are widely studied for biomedical applications. This paper reports on semi-interpenetrating network (IPN) hydrogels composed of poly(methacrylic acid) (PMA) and natural polymers (gelatin, alginate, and chitosan), synthesized via thermally-induced free-radical polymerization. The resulting hydrogels were evaluated for their physicochemical, mechanical, and drug release properties. Characterization techniques, including Fourier transform infrared (FTIR) spectroscopy, Field emission scanning electron microscope (FE-SEM), and swelling capacity analysis, demonstrated effective integration of natural polymers within the PMA network and their impact on hydrogel performance. PMA's pH sensitivity, combined with natural polymers, supports its suitability for controlled drug delivery and tissue engineering. Mechanical testing showed that adding 40 wt% of gelatin significantly increased the compressive strength from 0.16 MPa in pristine PMA to 2.35 MPa for PMA/gelatin IPN hydrogel and increased the modulus from 0.006 to 0.027 MPa. Chitosan provided moderate mechanical improvements, while alginate showed limited effects at higher concentrations. Swelling analysis revealed that the addition of gelatin and alginate reduced the equilibrium swelling ratio (ESR), suggesting denser crosslinking within the hydrogel matrix. Due to its pH-sensitive properties, chitosan had increased ESR at lower pH levels, showing potential for enhanced drug release modulation. Ciprofloxacin release studies demonstrated ESR-dependent drug release kinetics. These findings suggest that the incorporation of natural polymers, particularly gelatin, optimizes mechanical properties, pH-responsive swelling, and biocompatibility, making these hydrogels promising candidates for controlled drug delivery and tissue engineering applications.

**Keywords:** IPN hydrogel; poly(methacrylic acid); natural polymers; drug release

## ПОЛУМЕШАНИ ВМРЕЖЕНИ ХИДРОГЕЛОВИ БАЗИРАНИ НА ПОЛИ(МЕТАКРИЛНА КИСЕЛИНА) И ПРИРОДНИ ПОЛИМЕРИ ЖЕЛАТИН, ХИТОЗАН И АЛГИНАТ ЗА ПОТЕНЦИЈАЛНА БИМЕДИЦИНСКА ПРИМЕНА

Хидрогеловите, познати по нивната висока хидратација, порозност и пропустливост, се широко проучувани за биомедицинска примена. Овој труд прикажува полумешани вмрежени хидрогелови (IPN) составени од поли(метакрилна киселина) (PMA) и природни полимери (желатин, алгинат и хитозан), синтетизирани преку термички индуцирана полимеризација со слободни радикали. Добиените хидрогелови беа оценети според нивните физикохемиски, механички и својства за ослободување на лекови. Карактеризацијата, вклучувајќи Фуриеова трансформациона инфрацрвена (FTIR) спектроскопија, скенирачка електронска микроскопија со емисија на поле (FE-SEM) и анализа на способноста за набабрување, покажа ефикасна интеграција на природните полимери во мрежата на PMA и нивното влијание врз перформансите на хидрогеловите. pH-чувствителноста на PMA, во комбинација со природните полимери, ја потврдува нејзината погодност за контролирано ослободување на лекови и за инженерство на ткива. Механичките тестирања покажаа дека додавањето на 40 % масен удел на желатин значително ја зголемува компресивната цврстина од 0,16 MPa кај чиста PMA на 2,35 MPa кај PMA/желатин IPN хидрогелот, како и модулот од 0,006 на 0,027 MPa. Хитозан покажа умерено механичко подобрување, додека алгинат имаше ограничено влијание при повисоки концентрации. Анализата на набабрувањето откри дека додавањето на желатин и алгинат го намалува

рамнотежниот коефициент на набабрување (ESR), што укажува на погуста вмреженост во матрицата на хидрогелот. Поради своите pH-чувствителни својства, хитозанот покажа зголемен ESR при пониски pH вредности, што укажува на потенцијал за подобра модулација на ослободувањето на лекови. Истражувањата за ослободување на ципрофлоксацин покажаа дека кинетиката на ослободување на лекот зависи од ESR. Овие наоди укажуваат дека вклучувањето на природни полимери, особено желатин, ги оптимизира механичките својства, pH-одговорното набабрување и биокompatibilноста, со што овие хидрогелови се потенцијални кандидати за контролирано ослободување на лекови и за примена во инженерство на ткива.

**Keywords:** IPN хидрогел; поли(метакрилна киселина); природни полимери; ослободување на лек

## 1. INTRODUCTION

Hydrogels, hydrophilic three-dimensional polymeric networks, are highly attractive for biomedical applications due to their porous and permeable structure, biocompatibility, and ability to incorporate cells and drugs. Poly(methacrylic acid) (PMA) is an anionic polymer often used for the formation of three-dimensional networks with a relatively high hydration capacity.<sup>1</sup> Due to the lateral carboxyl groups present in the structure, PMA hydrogels are pH-sensitive. Ionization of PMA's carboxyl groups above pH 4.3 introduces a negative charge, expanding the hydrogel structure.<sup>1,2</sup> Conversely, at pH lower than 4.3, ionization and negative charges are absent, promoting hydrogen bonds and hydrophobic interactions between polymer chains, which in turn leads to structural shrinkage.<sup>2</sup> In addition, hydrophobic interactions from the  $\alpha$ -methyl group in PMA stabilize hydrogen bonds, restrict water infiltration, and improve mechanical properties.<sup>3</sup>

Along with PMA hydrogels' pH sensitivity, which is crucial for biomedical applications, particularly in controlled drug release,<sup>4-7</sup> there exists the possibility for flexible adjustment of properties by varying the monomer, crosslinker, initiator concentrations, and monomer neutralization degree.<sup>8,9</sup> However, the lack of cell recognition sites and biodegradability, as well as the relatively poor mechanical properties, limits the application of single-network PMA hydrogels in biomedicine.

Recent advances focus on interpenetrating (IPN) network hydrogels to enhance mechanical integrity and tailor properties.<sup>10-12</sup> Natural polymers, derived from various sources such as plants, animals, and microorganisms, have found widespread use in a variety of biomedical applications. They serve as pharmaceuticals, tissue regeneration scaffolds, drug delivery systems, and imaging agents. The appeal of natural polymer-based scaffolds for tissue repair and regeneration lies in their similarity to the extracellular matrix, high biocompatibility, mechanical tunability, and substantial water holding capacity.<sup>13</sup> Combining natural polymers with PMA networks is anticipated to improve biological activity and mechanical

strength while imparting biodegradability to resulting hydrogels.

Gelatin, a natural polymer similar to collagen, is extensively used in biomedicine due to its cost-effectiveness, biocompatibility, and biodegradability. It contains Arg-Gly-Asp (RGD)-like sequences that support cellular activities.<sup>14</sup> However, the challenges associated with gelatin include low mechanical strength and rapid dissolution at physiological temperatures, necessitating the use of toxic crosslinkers that can compromise the hydrogels' integrity.<sup>15</sup>

Chitosan, Earth's second most abundant polysaccharide after cellulose, is valued for its biocompatibility, biodegradability, and antimicrobial properties. It serves diverse roles in biomedical, pharmaceutical, and environmental applications, including wound healing, drug delivery, water treatment, and food packaging.<sup>16</sup> Chitosan hydrogels come in diverse forms such as liquid gels, powders, beads, films, tablets, capsules, microspheres, microparticles, sponges, nanofibrils, textile fibers, and inorganic composites.<sup>17</sup>

Alginate, a seaweed-derived linear unbranched polysaccharide containing repeating units of 1,4-linked  $\beta$ -D-mannuronic acid and  $\alpha$ -L-guluronic acid, is renowned for its versatility in forming hydrogels.<sup>18</sup> Its reversible gelling properties in aqueous solutions arise from ionic interactions with divalent cations, such as calcium, barium, and magnesium, interacting with carboxylic acid moieties on the guluronic acid residues.<sup>19</sup> Ionically crosslinked alginate hydrogels have gained significant interest in applications like drug delivery, cell encapsulation, and tissue regeneration.<sup>19</sup> Despite promising outcomes in previous studies, achieving control over mechanical properties, swelling ratios, and degradation profiles in ionically crosslinked alginate hydrogels remains challenging.

Although combining natural polymers with PMA can enhance hydrogel properties compared to single-network hydrogels, research in this area remains limited. Few papers have explored PMA/gelatin IPN hydrogels. Gupta et al. utilized glutaraldehyde to crosslink PMA/gelatin granules for controlled glipizide release,<sup>20</sup> while Zhang et al. employed low-temperature photo-induced free-ra-

dical polymerization to create semi-IPN networks with gelatin and PMA, achieving excellent mechanical properties.<sup>11</sup> Our recent investigations have focused on three-dimensional PMA/gelatin IPN hydrogels for potential biomedical applications, demonstrating significant improvements in mechanical strength and biodegradability.<sup>9,21</sup>

Chitosan's cationic groups enable it to form polyelectrolyte complexes with polyanionic polymers like poly(acrylic acid) and PMA making them promising for controlled drug release applications due to their pH sensitivity.<sup>22</sup> However, literature on IPN hydrogels combining chitosan and PMA is sparse. Maity et al. have synthesized PMA/chitosan IPN hydrogels for dye adsorption, enhancing thermal stability and adsorption capacity.<sup>23</sup> Another study has combined chitosan with a copolymer of methacrylic acid (MA) and acrylamide to form IPN hydrogels via sequential polymerization.<sup>24</sup> These hydrogels showed reduced swelling and faster release kinetics compared to the copolymers, suggesting potential applications in controlled release systems.

Similarly, studies on PMA/alginate IPN hydrogels are limited. Sajeesh and Sharma developed PMA/alginate microparticles for insulin release, showing pH-dependent release behavior.<sup>25</sup> Another study reported PMA/alginate semi-IPN hydrogels responsive to stimuli like temperature, pH, and ionic strength. It has been demonstrated that these hydrogels have potential for applications in artificial muscles, sensors, and controlled release systems with electrical modulation.<sup>26,27</sup> Recently, Pal et al. synthesized alginate/poly(methacrylic-co-acrylic acid) hydrogels, ionically crosslinked by Fe<sup>2+</sup>/Fe<sup>3+</sup>.<sup>28</sup> These hydrogels demonstrated pH-dependent drug delivery kinetics, inhibitory activity against breast cancer MDA-MB-231 cells, and biocompatibility with HEK-293 cells.

In this work, we synthesized IPN hydrogels based on PMA and natural polymers: gelatin, chitosan, and alginate. The obtained hydrogels were characterized in terms of physicochemical, structural, and mechanical properties, with a focus on the properties important for biomedical applications, as well as in vitro drug release.

## 2. MATERIALS AND METHODS

### 2.1. Materials

Methacrylic acid (MA) (99.5 %) was supplied by Merck KGaA. Poly(ethylene glycol) diacrylate (PEGDA) ( $M_w = 700$  g/mol), sodium hydroxide (NaOH) ( $\geq 97.0$  %), Type B bovine skin gelatin (gel strength 225), sodium alginate, and chitosan (medium

molecular weight, 75–85 % deacetylated) were obtained from Sigma Aldrich. The initiator, 2,2'-azobis[2-(2-imidazolin-2-yl)propane]dihydrochloride (VA-044) (99.8 %) was supplied by Wako Pure Chemical Industries. All chemicals were used as received.

### 2.2. Methods

#### 2.2.1. Synthesis of IPN hydrogels

The synthesis of IPN hydrogels was performed through thermally induced free-radical polymerization of MA in the presence of a crosslinker (PEGDA) and a natural polymer. Specifically, 0.3 ml of MA, 0.1 ml of 2 M NaOH, 0.4 ml of 2 % PEGDA, 0.5 ml of distilled water, and a specified amount of natural polymer (Table 1) were mixed and stirred at 60 °C for 20 minutes. Afterward, 0.2 ml of 1 % VA-044 initiator was added to the mixture, which was stirred for an additional 3 minutes before being poured into cylindrical molds (8 mm diameter). The molds were then placed in a dryer at 70 °C for 3 hours to allow polymerization. The resulting hydrogels were carefully removed from the molds and cut into 5 mm thick disks, which were then prepared for subsequent characterization tests. Hydrogels containing the drug ciprofloxacin were prepared in the same way, but with the addition of 10 mg of ciprofloxacin, and were labeled as PMA/CIP, PMAG3/CIP, PMAA3/CIP, and PMAC3/CIP.

Table 1

Sample codes and the content of natural polymer in the reaction mixture

Samples	Natural polymer	Mass (g)
PMA	/	/
PMAG1	gelatin	0.070
PMAG2	gelatin	0.140
PMAG3	gelatin	0.200
PMAC1	chitosan	0.007
PMAC2	chitosan	0.014
PMAC3	chitosan	0.020
PMAA1	alginate	0.007
PMAA2	alginate	0.014
PMAA3	alginate	0.020

#### 2.2.2. Fourier transform infrared (FTIR) spectroscopy analysis

Fourier transform infrared (FTIR) spectra of the samples were recorded in absorbance mode using a Nicolet™ iS™10 FTIR Spectrometer (Thermo

Fisher Scientific) with Smart iTR™ attenuated total reflectance (ATR) sampling accessories, within the range of 400–4000 cm<sup>-1</sup>, at a resolution of 4 cm<sup>-1</sup> using over 20 scan modes.

### 2.2.3. Degree of monomer conversion into gel phase

The degree of monomer conversion (*DC*) into gel phase was determined using the equation:

$$DC = \frac{m_0}{m_t} \quad (1)$$

where  $m_0$  is the weight of xerogel obtained by drying of hydrogels to constant mass after 24 h of swelling in phosphate-buffered saline (PBS) at pH = 7.4 and  $t = 37$  °C, during which unpolymerized molecules were rinsed out; and  $m_t$  is the theoretical mass of the xerogel obtained by summing all components constituting the polymer network.

### 2.2.4. Determination of swelling capacity

The equilibrium swelling ratio (ESR) was determined after 24 hours of immersion in different buffer solutions (0.01 M) – hydrochloric acid buffer (pH 1.2), acetate buffer (pH 4.0), and phosphate buffer (pH 7.4). The ESR was calculated using the following equation:

$$\text{ESR (\%)} = \frac{m_{eq}}{m_0} \quad (2)$$

where  $m_{eq}$  is the weight of the swollen hydrogel sample at equilibrium, and  $m_0$  is the weight of the xerogel. For each sample, at least three swelling measurements were performed, and the mean values were used.

### 2.2.5. Morphological investigations

A field emission scanning electron microscope (FE-SEM), Tescan MIRA 3 XMU (Czech Republic), operating at 20 kV, was used to characterize the morphology of the hydrogels. Prior to examination, all samples were swollen to equilibrium in PBS, lyophilized, and sputter-coated with gold using a POLARON SC502 sputter coater (United Kingdom) to avoid electrostatic charging. To prepare the samples for lyophilization, the samples were frozen at –80 °C for 1 h before the procedure. The solidified scaffolds were then transferred into a freeze-dryer (Beta 2–8 LD plus, Martin Christ, GmbH, Germany) and dried at –60 °C (at pressure of 0.011 mbar) for 24 h and at –75 °C

(at pressure of 0.0012 mbar) for an additional hour to remove the residual water.

### 2.2.6. Mechanical properties

The mechanical properties of hydrogels were evaluated using a universal testing machine AG-Xplus (Shimadzu, Japan), equipped with a 1000 N force load cell (force range from 0.01 to 1000 N). Before testing, the hydrogels were equilibrated in PBS at 37 °C and shaped into cylindrical specimens measuring 10 mm in height and 5 mm in diameter. Unconfined compression was performed up to 100 % deformation at a compression speed of 3 mm/min. Automatic detection of the contact between the plate and hydrogel was performed by setting a contact force of 0.1 N. The values of compressive strength were determined as stress values at fracture. The compressive modulus was calculated as the slope of the stress-strain curve from the linear region between 0 % and 10 % strain. At least three specimens were tested for each hydrogel, and the mean values and standard deviations were calculated.

### 2.2.7. In vitro drug release

Pristine PMA, PMAG3, PMAA3, and PMAC3 hydrogels, with and without ciprofloxacin, were cut into circular discs (10 mm in diameter, 5 mm in thickness). The hydrogels without the incorporated antibiotic served as controls. For the in vitro ciprofloxacin release study, a certain amount of the tested hydrogels (PMA/CIP, PMAG3/CIP, PMAA3/CIP, PMAC3/CIP) was immersed into 30 ml of PBS solution (pH 7.4) in a thermostatic incubator at 37 °C. At predetermined time intervals of 0.5, 1, 2, 4, 8, 24, 30, and 48 h, 2 ml of the release medium was sampled and replaced with fresh PBS to maintain sink conditions. Ciprofloxacin release was quantified using UV spectrophotometry (UV-1800 UV-VIS spectrophotometer, Shimadzu, Japan) at 270 nm, and cumulative release was calculated from a standard calibration curve. The release behaviors were assessed in triplicate, with results reported as mean ± standard deviation.

### 2.2.8. Drug release kinetic studies

To study the kinetics of the ciprofloxacin release, the results of in vitro tests were fitted to various kinetic models, including:

- Zero-order model:  $Q_t = Q_0 + K_0t$ , where  $Q_t$  is the amount of drug released in time  $t$ ,  $Q_0$  is the initial amount of drug in the solution, and  $K_0$  is the release constant;





**Fig. 2.** Photograph of the synthesized PMA, PMAG, PMAA, and PMAC hydrogels

For example, the reduced transparency in PMA/gelatin hydrogels was attributed to microscale phase separations due to hydrophobic interactions.<sup>21,29</sup> In contrast, the increase in alginate content in PMAA hydrogels led to reduced compactness. While PMAA1 and PMAA2 were mechanically stable, PMAA3 was softer and weaker. Hydrogels with even higher alginate content (not shown) were overly soft and prone to disintegration, likely due to hindered polymerization and crosslinking of the PMA network, resulting in insufficiently crosslinked, soft hydrogels.

### 3.2. Polymerization degree

The degree of conversion (DC) directly affects the physical and mechanical properties of hydrogels, indicating the extent of monomer incorporation. In this study, DC varied with the type of natural polymer used (Fig. 3).

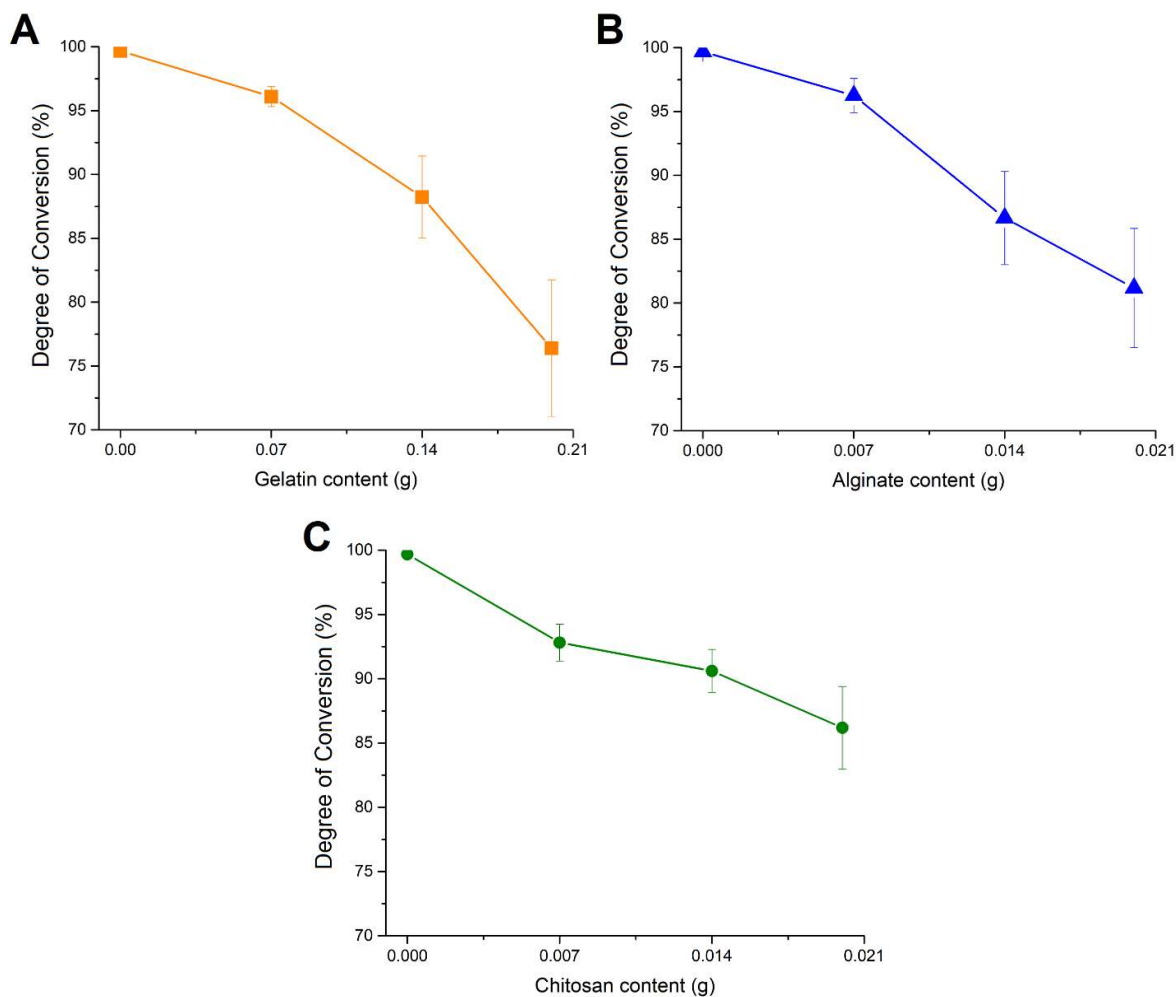


**Fig. 3.** The influence of natural polymer content on DC for PMAG (A), PMAA (B), and PMAC (C) hydrogels

For PMAG hydrogels, DC ranged from  $99.68 \pm 0.31\%$  to  $76.39 \pm 5.34\%$ , while PMAA hydrogels had a range of  $99.68 \pm 0.31\%$  to  $81.17 \pm 4.67\%$ , and PMAC hydrogels ranged from  $99.68 \pm 0.31\%$  to  $86.17 \pm 3.21\%$ . As natural polymer content increased, DC decreased due to higher viscosity of the reaction mixture and reduced monomer mobility, as well as physical interactions with the natural polymer's functional groups. PMAG3 had the lowest DC (75 %) due to the high gelatin content, but remained compact and functional, showing that higher natural polymer content can offset lower DC. In PMAA hydrogels, adding 0.02 g of alginate reduced the DC to 80 %, while higher alginate concentrations resulted in overly soft, non-functional hydrogels (data not shown). PMAC hydrogels showed a DC reduction to 86.2 % with 0.02 g of chitosan; however, higher chitosan content (not shown) still resulted in compact, functional hydrogels. This suggests that while natural polymers affect conversion and mechanical properties, careful optimization of the synthesis parameters, i.e., PMA to natural polymer ratio, monomer and polymer content, etc., can result in the formation of hydrogels with desirable characteristics.

### 3.3. Chemical structure of the semi-IPN hydrogels

The FTIR spectra of pristine PMA, gelatin, sodium alginate, chitosan, and the IPN hydrogels are presented in Figure 4. The spectrum of pristine PMA exhibited a strong peak at  $1691\text{ cm}^{-1}$ , corresponding to the C=O stretching of carboxylic groups. In the fingerprint region ( $600\text{--}1500\text{ cm}^{-1}$ ), smaller peaks at  $1534$  and  $1388\text{ cm}^{-1}$  were observed, indicating the asymmetric and symmetric stretching of carboxylate ions, respectively. Peaks at  $1478$  and  $1448\text{ cm}^{-1}$  corresponded to  $\text{CH}_3$  bending and  $\text{CH}_2$  scissoring.

The gelatin FTIR spectrum featured significant peaks at  $1628$ ,  $1522$ , and  $1235\text{ cm}^{-1}$  linked to the polypeptide backbone and amide vibrations. A broad peak at  $3275\text{ cm}^{-1}$  represented  $\text{-NH}$  and  $\text{-OH}$  stretching modes, the peak at  $3071\text{ cm}^{-1}$   $\text{-NH}$  stretching, while peaks at  $2935$  and  $2874\text{ cm}^{-1}$  were assigned to C–H stretching vibrations.

The PMAG3 IPN hydrogel showed characteristic bands for both components, gelatin and PMA. Increasing PMA content enhanced the intensity of the carboxylic C=O peak, while reducing the polypeptide C=O peak. Notably, the peaks corresponding to the amide C=O stretch ( $1628\text{ cm}^{-1}$ ) and the carboxyl groups of PMA ( $1691\text{ cm}^{-1}$ ) merged, forming a broader peak centered at  $1654\text{ cm}^{-1}$ , indicating interactions between PMA and gelatin. Additionally, a shift in the  $\text{-NH}$  bending vibration (from  $1522$  to

$1528\text{ cm}^{-1}$ ) further suggested the formation of mutual interactions, probably through hydrogen bonding.

The FTIR spectrum of chitosan displayed several characteristic absorption peaks: a strong band between  $3291\text{--}3361\text{ cm}^{-1}$  for N–H and O–H stretching, and bands at  $2921$  and  $2877\text{ cm}^{-1}$  for C–H symmetric and asymmetric stretching.<sup>30</sup> Bands at  $1645\text{ cm}^{-1}$  (amide I, C=O stretching),  $1325\text{ cm}^{-1}$  (amide III, C–N stretching), and  $1550\text{ cm}^{-1}$  (amide II, N–H bending) confirmed the presence of residual N-acetyl groups. A band at  $1589\text{ cm}^{-1}$  indicated N–H bending of the primary amine.

In the FTIR spectrum of the pure alginate hydrogel, the peaks at  $3240\text{ cm}^{-1}$  and  $2921\text{ cm}^{-1}$  corresponded to O–H and C–H bond stretching, respectively. Bands at  $1593\text{ cm}^{-1}$  and  $1405\text{ cm}^{-1}$  were attributed to the asymmetric and symmetric stretching of the carboxylate group ( $\text{COO}^-$ ). The bands at  $1023\text{ cm}^{-1}$  and  $1081\text{ cm}^{-1}$  were associated with C–O stretching, while peaks at  $946\text{ cm}^{-1}$ ,  $883\text{ cm}^{-1}$ , and  $1081\text{ cm}^{-1}$  confirmed the presence of guluronic and mannuronic acid units. The band at  $810\text{ cm}^{-1}$  indicated Na–O bonds in sodium alginate.<sup>31</sup>

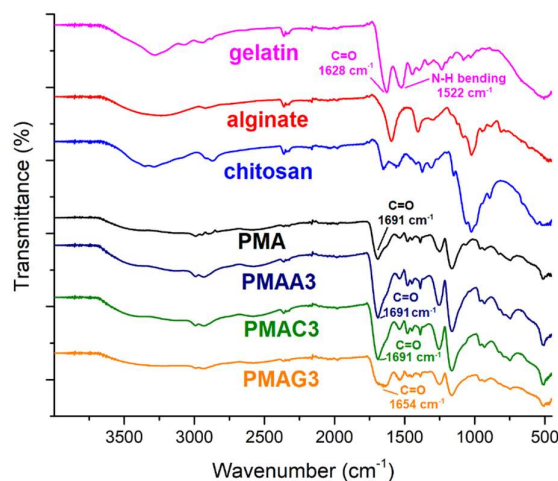
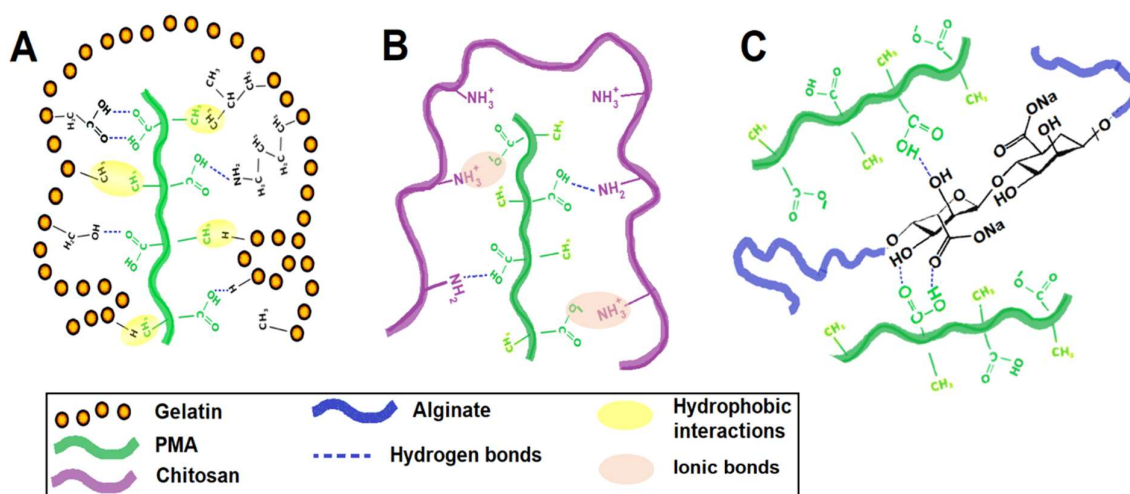


Fig. 4. FTIR spectra of natural polymers, PMA, and IPN hydrogels

The spectra of the PMAC3 and PMAA3 hydrogels were almost identical to that of the pure PMA hydrogel, with no distinct features matching the alginate or chitosan spectra. This suggests that the addition of 0.02 g of chitosan or alginate was insufficient relative to the mass of PMA to produce measurable spectral changes, and probably the main absorption peaks of chitosan blended with the peaks of PMA. The change in transparency of PMA hydrogels upon the addition of chitosan confirmed the establishment of mutual interactions. Maiti et al.

have studied PMA/chitosan IPN hydrogels for dye absorption applications and reported shifts in the vibrational frequencies of functional groups in both PMA and chitosan after IPN formation.<sup>23</sup> However, the main absorption peaks related to PMA functional groups showed minimal shifts, consistent with our findings. Although the chitosan content was insufficient to induce major spectral changes, possible interactions based on the structure of the components

in the PMA/chitosan system included: 1) hydrogen bonding between chitosan and PMA; 2) electrostatic interactions between the positively charged ammonium groups of chitosan and the negatively charged carboxylate ions of PMA; and 3) hydrophobic interactions.<sup>32</sup> Figure 5 illustrates the proposed interactions between PMA and natural polymer molecules within the hydrogels' structures.



**Fig. 5.** Proposed interactions between PMA and natural polymers within the structures of PMAG (A), PMAC (B), and PMAA (C) hydrogels

### 3.4. Swelling and pH sensitivity

Swelling ability is a crucial characteristic of pH-sensitive hydrogels in drug delivery applications, as it can significantly influence the release profiles of bioactive molecules.<sup>33</sup> In addition, the degree of hydrogel swelling is an essential parameter for various medical applications, particularly when hydrogel-based devices are implanted near pressure-sensitive tissues and organs, such as in spinal or brain surgery.<sup>34</sup> In this study, we investigated the swelling behavior of hydrogels across a pH range of 1.2 to 7.4 at 37 °C. The equilibrium swelling ratio (ESR) as a function of natural polymer content for hydrogels under different pH conditions is illustrated in Figures 6A–C.

All hydrogels demonstrated pH-sensitive swelling behavior. At pH 1.2 and 4.0, which are below the  $pK_a$  value of PMA (approximately 4.3), the ESR was low for all hydrogels. When the pH exceeded the  $pK_a$ , the carboxylic groups became ionized, resulting in repulsive forces between the negatively charged carboxylate ions and an increased ionic density, which contributed to a higher ESR. However, an increase in the natural polymer

content led to a greater degree of crosslinking, resulting in a lower ESR. For instance, for PMAG at pH 7.4, the ESR decreased from 15.9 to 3.4 g/g as gelatin content increased from 0.0 to 0.2 g (Figure 6A). Similarly, for PMAA and PMAC, the ESR decreased from 15.9 to 8.5 (Figure 6B) and 7.3 g/g (Fig. 6C), respectively. These ESR decreases indicate that the addition of gelatin to PMA hydrogels produced the most compact and highly crosslinked structure compared to alginate and chitosan.

Interestingly, although PMAC exhibited a lower ESR at pH 7.4 compared to PMAA, it demonstrated significantly higher ESR under acidic conditions, which increased further with higher chitosan content (3.66 g/g for PMAC3 and 1.41 g/g for PMAA3). This behavior is attributed to the pH sensitivity of chitosan, stemming from the presence of amino groups that can be protonated or deprotonated depending on the surrounding pH. At low pH levels, the chitosan amino groups became protonated, resulting in a positively charged structure that enhanced swelling and solubility, as also reported in another study.<sup>35</sup>

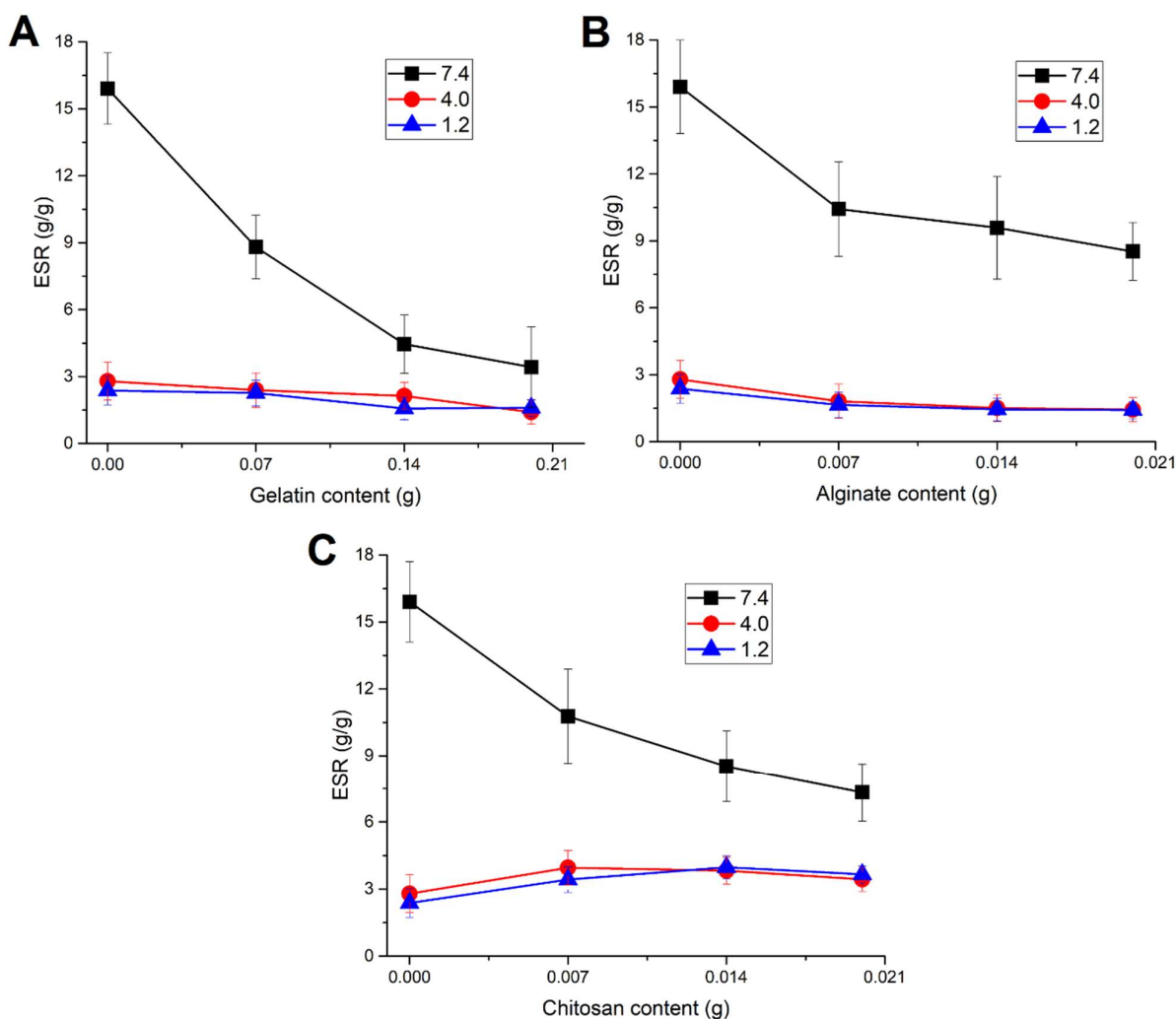


Fig. 6. pH sensitivity of natural polymer content on ESR for PMAG (A), PMAA (B), and PMAC (C) hydrogels

### 3.5. Field emission scanning electron microscopy

Figure 7 shows cross-sectional FE-SEM images of lyophilized, swollen hydrogels, revealing distinct microstructural characteristics due to the different natural polymers used for IPN formation. Pristine PMA exhibited a highly porous structure with pore sizes up to 500  $\mu\text{m}$ . The addition of gelatin significantly reduced porosity, with PMAG3 showing more uniform microstructure and a smaller average pore size of approximately 10  $\mu\text{m}$ . In contrast, the addition of alginate and chitosan had less effect on the porosity, with pore sizes ranging from 100 to 500  $\mu\text{m}$ . The PMAA3 hydrogel displayed a highly irregular microstructure, probably due to interruptions in the polymerization process. PMAC3,

however, had a relatively uniform microstructure, similar to pristine PMA.

These observations correlate with ESR results, as the microstructure is strongly influenced by water content. Specifically, porosity and pore size are directly related to the amount of water in the structure, as well as the formation of ice crystals during the freezing process. On the other hand, the ESR is influenced by the polymerization process and the degree of crosslinking, meaning that the network parameters, such as the density of crosslinks, play a crucial role in shaping the final microstructure. Thus, both the water content and the synthesis parameters (type and content of natural polymer) significantly contributed to the development of the hydrogel's porosity and overall architecture.

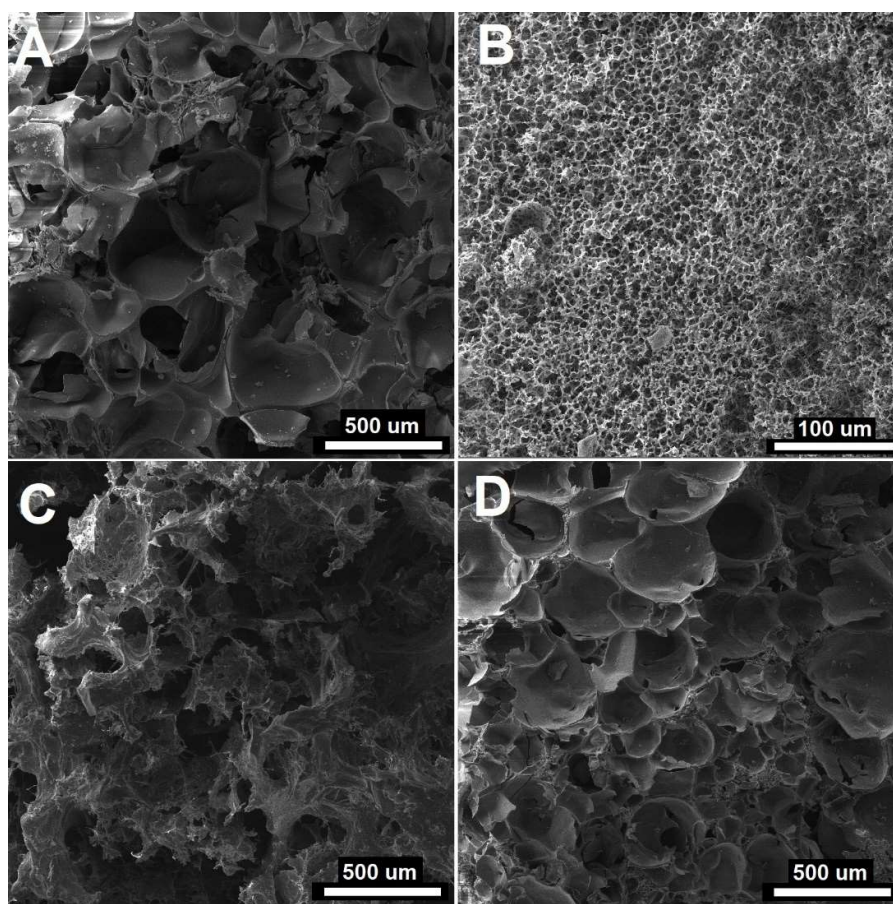


**Fig. 7.** Microstructure of the lyophilized hydrogels: PMA (A), PMAG3 (B), PMAA3 (C), and PMAC3 (D)

### 3.6. Mechanical properties

The mechanical properties of hydrogels are vital for their performance in applications like tissue engineering and drug delivery, as they ensure stability, durability, and functionality under operational conditions. Optimizing mechanical performance is essential for ensuring the functionality and longevity of hydrogels in their intended applications. Figures 8A–F illustrate the stress-strain curves, as well as the trends in modulus and compressive strength, as a function of natural polymer content. Notable improvements in compressive mechanical properties were observed for PMAG (Fig. 8A) and PMAC (Fig. 8C) hydrogels with increasing gelatin and chitosan content. Specifically, the addition of 0.2 g of gelatin (PMAG3) enhanced the compressive strength of PMA hydrogels from 0.16 MPa to 2.35 MPa (Figure 8D), representing a roughly 15-fold increase. Similarly, the modulus increased from 0.006 MPa to 0.027 MPa, a four-fold improvement.

In contrast, the mechanical enhancements due to chitosan incorporation were less pronounced. At

the maximum tested chitosan content, compressive strength and modulus increased by factors of two and four, respectively, compared to pristine PMA hydrogels (Fig. 8F). These results indicate that the incorporation of natural polymers into PMA hydrogels enhanced their mechanical properties, due to the formation of a semi-interpenetrating polymer network (semi-IPN). The presence of the interpenetrant (natural polymer) improved the crosslinking, increasing the number of chain entanglements and forming physical bonds with PMA.

The stronger mechanical improvements observed with gelatin can be attributed to the high number of hydrogen bonds and hydrophobic interactions present within the material, as well as the significantly lower water content in the structure as a consequence of these interactions. The abundance of microphase-separated hydrophobic domains acted as permanent crosslinks, alongside the chemical crosslinks formed by PEGDA.<sup>29</sup> These hydrophobic domains resulted from the  $\alpha$ -methyl groups in PMA interacting with the hydrophobic regions of gelatin. In contrast, poly(acrylic acid) (PAA)-based hydro-

gels, which lack these interactions, have exhibited significantly lower mechanical properties.<sup>21</sup> This highlights the crucial role of hydrophobic interactions in PMA/gelatin systems. Additionally, hydrogen bonds between the carboxylic groups of PMA and the hydrophilic groups of gelatin contributed to dense dynamic crosslinking, enabling much higher tensile strength and deformation compared to pristine PMA hydrogels. Also, since a huge part of the structure of the hydrogels was water, which acts as a plasticizer, reducing the water content in the structure of the

hydrogels additionally contributed to better mechanical properties.

While chitosan enhanced the mechanical properties of PMA hydrogels, its effect was less pronounced compared to gelatin. This difference can be attributed to the weaker interactions between chitosan and PMA, as confirmed by FTIR analysis, which provided minimal contribution to mechanical reinforcement. Furthermore, the significantly higher ESR relative to PMAG hydrogels negatively contributed to the overall mechanical performance.

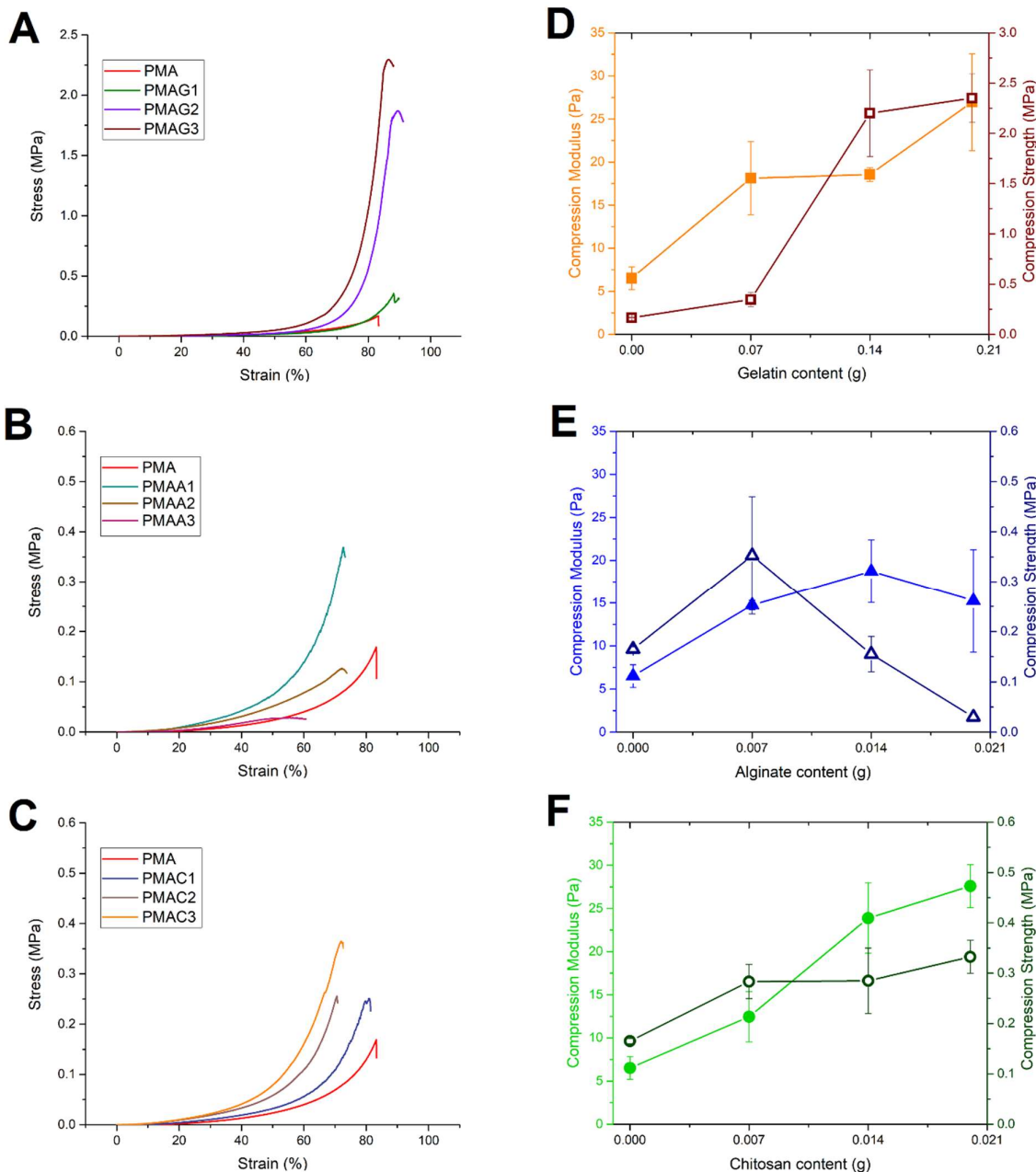


**Fig. 8.** Stress-strain curves for IPN hydrogels with different contents of natural polymers: gelatin (A), alginate (B), and chitosan (C). The influence of natural polymer content on mechanical properties of PMAG (D), PMAA (E), and PMAC (F) hydrogels

Increasing the alginate content initially enhanced both compressive strength and modulus, with optimal values observed for PMAA1 and PMAA2 samples, i.e., 0.014 g and 0.007 g of alginate, respectively (Fig. 8E). However, further increases in alginate concentration led to a decline in mechanical properties. At lower concentrations, alginate probably promoted crosslinking through hydrogen bonding between its hydroxyl groups and the carboxyl groups of PMA, which strengthened the hydrogel network. In contrast, higher alginate concentrations hindered the polymerization process, weakening the overall structure. When alginate content exceeded 0.02 g (PMAA3), the polymerization was significantly impaired, resulting in a very soft, poorly structured hydrogel that was difficult to manipulate.

In summary, the addition of natural polymers, particularly gelatin, significantly improved the mechanical properties of PMA hydrogels through enhanced crosslinking and lowered water content in the structure, while alginate's effect was more limited and became detrimental at higher concentrations.

### 3.7. *In vitro* release of ciprofloxacin from PMA/CIP, PMAG3/CIP, PMAA3/CIP, and PMAC3/CIP hydrogels

The ciprofloxacin release profiles from different hydrogels – PMA, PMAG3, PMAA3, and PMAC3 – were observed over a 48-hour period under simulated physiological conditions (PBS at 37 °C) and are presented in Figure 9. The release kinetics were influenced by the swelling and diffusion properties of the hydrogels. PMA, which exhibited the highest ESR, demonstrated the greatest drug release, whereas PMAG3, PMAA3, and PMAC3, with lower ESR values, released comparatively lower amounts of the drug.

The initial release (within the first hour) was relatively low across all hydrogels. Specifically, PMA released  $5.1 \pm 0.6$  % of the ciprofloxacin, while PMAG3, PMAA3, and PMAC3 released  $3.5 \pm 1.1$  %,  $4.1 \pm 1.8$  %, and  $4.3 \pm 0.2$  %, respectively. In the subsequent hours, the hydrogels continued to release the drug, with PMA showing a significantly higher release ( $30.8 \pm 0.7$  %) by 7 hours, compared to  $20.9 \pm 2.1$  %,  $22.5 \pm 5.0$  %, and  $26.2 \pm 5.1$  % for the PMAG3, PMAA3, and PMAC3 hydrogels, respectively.

By the 24-hour mark, the drug release from PMA reached  $63.0 \pm 0.4$  %, while PMAG3, PMAA3, and PMAC3 released  $42.9 \pm 6.3$  %,  $48.4 \pm 5.3$  %, and  $48.8 \pm 6.1$  % of the drug, respectively. These differences can be attributed to the varying ESR values: PMA, with its higher ESR, likely swells more, creating larger voids for the drug to diffuse

through, thus allowing for a higher cumulative release. In contrast, the IPN hydrogels with lower ESR values – PMAG3, PMAA3, and PMAC3 – exhibited reduced swelling, which restricted the diffusion of the drug and resulted in slower release.

After 48 hours, PMA had released  $82.4 \pm 2.9$  % of the ciprofloxacin, significantly more than the other hydrogels, which released  $62.1 \pm 4.2$  %,  $67.7 \pm 6.7$  %, and  $68.1 \pm 6.4$  % of the drug. These results underscore the critical role of the hydrogel's swelling behavior in modulating drug release kinetics. These findings also highlight the impact of the natural polymer type on drug release. The differences in release profiles suggest that a polymer's swelling behavior and water interaction can be tailored to control release kinetics. Thus, selecting the right polymer is crucial for designing a hydrogel network that provides precise, controlled drug delivery to meet specific therapeutic needs.

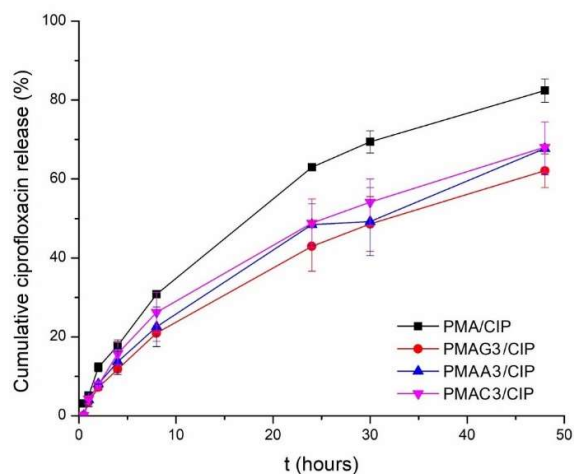


Fig. 9. Cumulative release of ciprofloxacin from PMA/CIP, PMAG3/CIP, PMAA3/CIP, and PMAC3/CIP hydrogels in PBS

To establish the ciprofloxacin release profiles from hydrogels, the *in vitro* ciprofloxacin release test results were fitted to mathematical models – zero-order and first-order models, as well as the Higuchi model.<sup>36</sup> The correlation coefficient ( $r^2$ ) between the model-predicted and experimentally obtained values, determined through regression analysis, served as the criterion for selecting the kinetic model that best fits the drug release kinetics. The correlation coefficient values ( $r^2$ ) for all the tested models, presented in Table 2, indicate which kinetic model aligns most closely with the experimental data.

Table 2

The correlation coefficient ( $r^2$ ) values for the zero-order, first-order, and Higuchi model

Sample	Zero-order model ( $r^2$ )	First-order model ( $r^2$ )	Higuchi model ( $r^2$ )
PMA/CIP	0.93	0.92	0.99
PMAG3/CIP	0.89	0.93	0.99
PMAA3/CIP	0.91	0.90	0.99
PMAC3/CIP	0.93	0.92	0.99

The Higuchi model exhibited the highest  $r^2$  values for the samples, indicating that ciprofloxacin diffusion from hydrogels followed the Higuchi model. The regression equation for the Higuchi model had the form:

$$Q_t = 13.5 t^{1/2} - 7.2 \quad (r^2 = 0.99, \text{ sample PMA/CIP}) \quad (3)$$

$$Q_t = 10.1 t^{1/2} - 7.2 \quad (r^2 = 0.99, \text{ sample PMAG3/CIP}) \quad (4)$$

$$Q_t = 10.8 t^{1/2} - 7.4 \quad (r^2 = 0.99, \text{ sample PMAA3/CIP}) \quad (5)$$

$$Q_t = 11.05 t^{1/2} - 6.7 \quad (r^2 = 0.99, \text{ sample PMAC3/CIP}) \quad (6)$$

where  $Q_t$  represents the amount of ciprofloxacin dissolved at time  $t$ , and  $K_H$  is the Higuchi release constant. In a Higuchi model of drug release, the drug is released in a manner that is primarily diffusion-controlled and proportional to the square root of time, meaning that the amount of drug released increases gradually over time, following a quadratic relationship. The Higuchi model suggests that the release occurs sustainably, where the drug diffuses through the hydrogel matrix into the surrounding medium. This model is particularly useful for describing systems where sustained and controlled drug release is desired, such as hydrogels used for therapeutic applications. According to the Higuchi model, these systems can provide a prolonged therapeutic effect while minimizing the risk of toxicity associated with rapid release.

#### 4. CONCLUSION

The manuscript concludes that incorporating natural polymers into PMA hydrogels can significantly enhance their suitability for biomedical applications, particularly in controlled drug delivery and tissue engineering. Through the development of semi-IPN hydrogels with PMA and gelatin, chito-

san, and alginate, the study demonstrated how natural polymer integration influences key properties, including mechanical strength, swelling behavior, and drug release profiles.

Mechanical testing revealed that gelatin markedly improved the hydrogel's compressive strength and modulus, suggesting a stronger and more durable structure. This improvement is attributed to enhanced crosslinking and network density when gelatin is introduced. Chitosan provided moderate mechanical benefits, while alginate exhibited minimal effects on mechanical properties at higher concentrations, suggesting that gelatin is particularly effective in strengthening the hydrogel matrix.

Swelling analysis showed that all hydrogels displayed pH-sensitive swelling behavior while the addition of natural polymers reduced the ESR, indicating a denser crosslinked network. In acidic conditions, chitosan-based hydrogels exhibited higher ESR due to the protonation of amino groups. Demonstrated pH responsiveness is beneficial for drug delivery applications, as it can enable controlled release in response to environmental pH changes.

Ciprofloxacin release studies further highlighted the role of natural polymers in modifying release kinetics. Gelatin-modified hydrogels exhibited a slower release profile compared to chitosan and alginate variants, due to their more crosslinked structure, lower porosity, and reduced swelling; however, all modified hydrogels showed significantly slower release rates than pristine PMA. This behavior supports the development of drug delivery systems tailored to specific pH conditions, aligning with the requirements for targeted and sustained drug release.

Overall, the study demonstrates that natural polymer integration, particularly with gelatin, enhances the mechanical properties, pH-sensitive swelling, and controlled drug release potential of PMA-based hydrogels. These findings support the development of advanced hydrogel systems for biomedical applications, as the optimized mechanical strength, tunable swelling, and drug release capabilities present promising prospects for effective and adaptable drug delivery and tissue engineering solutions.

**Acknowledgements:** Research was supported by the Science Fund of Republic of Serbia, #GRANT No. 7470, „Novel hybrid biomimetic macroporous composites with tuned biodegradability, improved osteointegration and anticancer properties for bone tissue regeneration – HyBioComBone” and Ministry of Science, Technological Development and Innovation, Republic of Serbia (Contracts No. 451-03-66/2024-03/200287 and 451-03-65/2024-03/200135).

#### REFERENCES

- (1) Zhang, J.; Peppas, N. A., Synthesis and Characterization of PH- and Temperature-Sensitive Poly(Methacrylic Acid)/

- Poly(N-Isopropylacrylamide) Interpenetrating Polymeric Networks. *Macromolecules* **2000**, *33* (1), 102–107. <https://doi.org/10.1021/ma991398q>
- (2) Xue, R.; Zhang, W.; Sun, P.; Zada, I.; Guo, C.; Liu, Q.; Gu, J.; Su, H.; Zhang, D., Angle-Independent PH-Sensitive Composites with Natural Gyroid Structure. *Sci. Rep.* **2017**, *7*, 42207. <https://doi.org/10.1038/srep42207>
  - (3) Gulyuz, U., Dual Cross-Linked Polymethacrylic Acid Hydrogels with Tunable Mechanical Properties and Shape Memory Behavior. *Macromol. Mater. Eng.* **2021**, *306* (9), 2100201. <https://doi.org/10.1002/mame.202100201>
  - (4) Lumbreras-Aguayo, A.; Meléndez-Ortiz, H. I.; Puente-Urbina, B.; Alvarado-Canché, C.; Ledezma, A.; Romero-García, J.; Betancourt-Galindo, R., Poly(Methacrylic Acid)-Modified Medical Cotton Gauzes with Antimicrobial and Drug Delivery Properties for Their Use as Wound Dressings. *Carbohydr. Polym.* **2019**, *205*, 203–210. <https://doi.org/10.1016/j.carbpol.2018.10.015>
  - (5) Caldorera-Moore, M.; Vela Ramirez, J. E.; Peppas, N. A., Transport and Delivery of Interferon- $\alpha$  through Epithelial Tight Junctions via pH-Responsive Poly (Methacrylic Acid-Grafted-Ethylene Glycol) Nanoparticles. *J. Drug Target.* **2019**, *27* (5–6), 582–589. <https://doi.org/10.1080/1061186X.2018.1547732>
  - (6) Pérez-Chávez, N. A.; Nosthas Aguiar, V.; Allegretto, J. A.; Albasa, A. G.; Giussi, J. M.; Longo, G. S., Triggering Doxorubicin Release from Responsive Hydrogel Films by Polyamine Uptake. *Soft Matter* **2020**, *16* (32), 7492–7502. <https://doi.org/10.1039/D0SM00951B>
  - (7) Vatankhah, Z.; Dehghani, E.; Salami-Kalajahi, M.; Roghani-Mamaqani, H., One-Step Fabrication of Low Cytotoxic Anisotropic Poly(2-Hydroxyethyl Methacrylate-Co-Methacrylic Acid) Particles for Efficient Release of DOX. *J. Drug Deliv. Sci. Technol.* **2019**, *54*, 101332. <https://doi.org/10.1016/j.jddst.2019.101332>
  - (8) Panic, V.; Adnadjevic, B.; Velickovic, S.; Jovanovic, J., The Effects of the Synthesis Parameters on the Xerogels Structures and on the Swelling Parameters of the Poly(Methacrylic Acid) Hydrogels. *Chem. Eng. J.* **2010**, *156* (1), 206–214. <https://doi.org/10.1016/J.CEJ.2009.10.040>
  - (9) Ugrinovic, V.; Panic, V.; Spasojevic, P.; Seslija, S.; Bozic, B.; Petrovic, R.; Janackovic, D.; Veljovic, D., Strong and Tough, pH Sensible, Interpenetrating Network Hydrogels Based on Gelatin and Poly (Methacrylic Acid). *Polym. Eng. Sci.* **2022**, *62* (3), 622–636. <https://doi.org/10.1002/pen.25870>
  - (10) Yan, X.; Chen, Q.; Zhu, L.; Chen, H.; Wei, D.; Chen, F.; Tang, Z.; Yang, J.; Zheng, J., High Strength and Self-Healable Gelatin/Polyacrylamide Double Network Hydrogels. *J. Mater. Chem. B* **2017**, *5* (37), 7683–7691. <https://doi.org/10.1039/C7TB01780D>
  - (11) Zhang, H. J.; Wang, L.; Wang, X.; Han, Q.; You, X., Developing Super Tough Gelatin-Based Hydrogels by Incorporating Linear Poly(Methacrylic Acid) to Facilitate Sacrificial Hydrogen Bonding. *Soft Matter* **2020**, *16* (20), 4723–4727. <https://doi.org/10.1039/D0SM00422G>
  - (12) Thangprasert, A.; Tansakul, C.; Thuaksubun, N.; Meesane, J., Mimicked Hybrid Hydrogel Based on Gelatin/PVA for Tissue Engineering in Subchondral Bone Interface for Osteoarthritis Surgery. *Mater. Des.* **2019**, *183*, 108113. <https://doi.org/10.1016/j.matdes.2019.108113>
  - (13) Ter Horst, B.; Moiemmen, N. S.; Grover, L. M., 6 – Natural Polymers: Biomaterials for Skin Scaffolds; In: Biomaterials for Skin Repair and Regeneration, E. García-Gareta, (Ed.). Woodhead Publishing, 2019; pp 151–192. <https://doi.org/10.1016/B978-0-08-102546-8.00006-6>
  - (14) Georgopoulou, A.; Papadogiannis, F.; Batsali, A.; Marakis, J.; Alpantaki, K.; Eliopoulos, A. G.; Pontikoglou, C.; Chatzinkolaidou, M., Chitosan/Gelatin Scaffolds Support Bone Regeneration. *J. Mater. Sci. Mater. Med.* **2018**, *29* (5), 59. <https://doi.org/10.1007/s10856-018-6064-2>
  - (15) Sung, H.; Huang, D.; Chang, W.; Huang, R.; Hsu, J., Evaluation of Gelatin Hydrogel Crosslinked with Various Crosslinking Agents as Bioadhesives: In Vitro Study. *J. Biomed. Mater. Res.* **1999**, *46* (4), 520–530.
  - (16) Bhattarai, N.; Gunn, J.; Zhang, M., Chitosan-Based Hydrogels for Controlled, Localized Drug Delivery. *Adv. Drug Deliv. Rev.* **2010**, *62* (1), 83–99. <https://doi.org/10.1016/j.addr.2009.07.019>
  - (17) Denkbaz, E. B.; Ottenbrite, R. M., Perspectives on: Chitosan Drug Delivery Systems Based on Their Geometries. *J. Bioact. Compat. Polym.* **2006**, *21* (4), 351–368. <https://doi.org/10.1177/08839115060066930>
  - (18) Jeon, O.; Bouhadir, K. H.; Mansour, J. M.; Alsberg, E., Photocrosslinked Alginate Hydrogels with Tunable Biodegradation Rates and Mechanical Properties. *Biomaterials* **2009**, *30* (14), 2724–2734. <https://doi.org/10.1016/j.biomaterials.2009.01.034>
  - (19) Coviello, T.; Matricardi, P.; Marianecchi, C.; Alhaique, F., Polysaccharide Hydrogels for Modified Release Formulations. *J. Control. Release* **2007**, *119* (1), 5–24. <https://doi.org/10.1016/j.jconrel.2007.01.004>
  - (20) Gupta, N. V.; Satish, C. S.; Shivakumar, H. G., Preparation and Characterization of Gelatin-Poly(Methacrylic Acid) Interpenetrating Polymeric Network Hydrogels as a pH-Sensitive Delivery System for Glipizide. *Indian J. Pharm. Sci.* **2007**, *69* (1), 64.
  - (21) Ugrinovic, V.; Markovic, M.; Bozic, B.; Panic, V.; Veljovic, D., Physically Crosslinked Poly(Methacrylic Acid)/Gelatin Hydrogels with Excellent Fatigue Resistance and Shape Memory Properties. *Gels* **2024**, *12* (7), 444. <https://doi.org/10.3390/gels10070444>
  - (22) Chen, S.; Liu, M.; Jin, S.; Chen, Y., Synthesis and Swelling Properties of pH-Sensitive Hydrogels Based on Chitosan and Poly(Methacrylic Acid) Semi-Interpenetrating Polymer Network. *J. Appl. Polym. Sci.* **2005**, *98* (4), 1720–1726. <https://doi.org/10.1002/app.22348>
  - (23) Maity, J.; Ray, S. K., Enhanced Adsorption of Methyl Violet and Congo Red by Using Semi and Full IPN of Polymethacrylic Acid and Chitosan. *Carbohydr. Polym.* **2014**, *104*, 8–16. <https://doi.org/10.1016/j.carbpol.2013.12.086>

- (24) Dragan, E. S.; Cocarta, A. I.; Gierszewska, M., Designing Novel Macroporous Composite Hydrogels Based on Methacrylic Acid Copolymers and Chitosan and in Vitro Assessment of Lysozyme Controlled Delivery. *Colloids Surfaces B Biointerfaces* **2016**, *139*, 33–41. <https://doi.org/10.1016/j.colsurfb.2015.12.011>
- (25) Sajeesh, S.; Sharma, C. P., Poly Methacrylic Acid-Alginate Semi-IPN Microparticles for Oral Delivery of Insulin: A Preliminary Investigation. *J. Biomater. Appl.* **2004**, *19* (1), 35–45. <https://doi.org/10.1177/0885328204042992>
- (26) Kim, S. J.; Yoon, S. G.; Kim, I. Y.; Kim, N. G.; Kim, S. I., Swelling Characterizations of the Interpenetrating Polymer Network Hydrogels Composed of Poly-methacrylic Acid and Alginate. *J. Macromol. Sci. Part A* **2005**, *42* (6), 811–820. <https://doi.org/10.1081/MA-200058669>
- (27) Kim, S. J.; Yoon, S. G.; Lee, Y. H.; Kim, S. I., Bending Behavior of Hydrogels Composed of Poly(Methacrylic Acid) and Alginate by Electrical Stimulus. *Polym. Int.* **2004**, *53* (10), 1456–1460. <https://doi.org/10.1002/pi.1560>
- (28) Pal, K.; Jaiswal, S.; Yadav, P.; Kumar, R.; Minocha, T.; Yadav, S. K., Multi-Responsive Hydrogel Based on Sodium Alginate with Acrylic Acid and Methacrylic Acid: Impact on Normal and Cancerous Cells. *J. Polym. Sci.* **2025**, *63* (3), 578–594. <https://doi.org/10.1002/pol.20240804>
- (29) Zhang, H. J.; Wang, X.; Yang, Y.; Sun, T. L.; Zhang, A.; You, X., Effect of Hydrophobic Side Group on Structural Heterogeneities and Mechanical Performance of Gelatin-Based Hydrogen-Bonded Hydrogel. *Macromolecules* **2022**, *55* (17), 7401–7410. <https://doi.org/10.1021/acs.macromol.2c01386>
- (30) Fernandes Queiroz, M.; Melo, K. R.; Sabry, D. A.; Sasaki, G. L.; Rocha, H. A., Does the Use of Chitosan Contribute to Oxalate Kidney Stone Formation? *Marine Drugs*. 2015, pp. 141–158. <https://doi.org/10.3390/md13010141>
- (31) Bekin, S.; Sarmad, S.; Gürkan, K.; Keçeli, G.; Gürdağ, G., Synthesis, Characterization and Bending Behavior of Electroresponsive Sodium Alginate/Poly(Acrylic Acid) Interpenetrating Network Films under an Electric Field Stimulus. *Sensors Actuators B Chem.* **2014**, *202*, 878–892. <https://doi.org/10.1016/j.snb.2014.06.051>
- (32) Chenite, A.; Chaput, C.; Wang, D.; Combes, C.; Buschmann, M. D.; Hoemann, C. D.; Leroux, J. C.; Atkinson, B. L.; Binette, F.; Selmani, A., Novel Injectable Neutral Solutions of Chitosan Form Biodegradable Gels in Situ. *Biomaterials* **2000**, *21* (21), 2155–2161. [https://doi.org/10.1016/S0142-9612\(00\)00116-2](https://doi.org/10.1016/S0142-9612(00)00116-2)
- (33) Rizwan, M.; Yahya, R.; Hassan, A.; Yar, M.; Azzahari, A. D.; Selvanathan, V.; Sonsudin, F.; Abouloula, C. N., pH Sensitive Hydrogels in Drug Delivery: Brief History, Properties, Swelling, and Release Mechanism, Material Selection and Applications. *Polymers (Basel)*. **2017**, *9* (4). <https://doi.org/10.3390/polym9040137>
- (34) Revete, A.; Aparicio, A.; Cisterna, B. A.; Revete, J.; Luis, L.; Ibarra, E.; Segura González, E. A.; Molino, J.; Reginensi, D., Advancements in the Use of Hydrogels for Regenerative Medicine: Properties and Biomedical Applications. *Int. J. Biomater.* **2022**, *2022* (1), 3606765. <https://doi.org/10.1155/2022/3606765>
- (35) Liu, Y.; Lang, C.; Ding, Y.; Sun, S.; Sun, G., Chitosan with Enhanced Deprotonation for Accelerated Thermosensitive Gelation with  $\beta$ -Glycerophosphate. *Eur. Polym. J.* **2023**, *196*, 112229. <https://doi.org/10.1016/j.eurpolymj.2023.112229>
- (36) Dash, S.; Murthy, P. N.; Nath, L.; Chowdhury, P., Kinetic Modeling on Drug Release from Controlled Drug Delivery Systems. *Acta Pol. Pharm.* **2010**, *67* (3), 217–223.